WP17ER-PR(18) 21459

M Fitzgerald et al.

HALO: A full-orbit model of nonlinear interaction of fast particles with eigenmodes

Preprint of Paper to be submitted for publication in
Computer Physics Communications

This work has been carried out within the framework of the EUROfusion Consortium and has received funding from the Euratom research and training programme 2014-2018 under grant agreement No 633053. The views and opinions expressed herein do not necessarily reflect those of the European Commission.

HALO: A full-orbit model of nonlinear interaction of fast particles with eigenmodes

M. Fitzgerald, J. Buchanan, R.J. Akers, B.N. Breizman, S.E. Sharapov

HALO (HAgis LOcust) solves the initial value Vlasov-Maxwell problem perturbatively for application to certain nonlinear wave-particle problems in tokamak plasmas. It uses the same basic approach as the HAGIS code (Pinches et al., 1998) for wave evolution but is built on the LOCUST-GPU full-orbit code (Akers et al., 2012) for the solution of the Hamiltonian fast particle motion in cylindrical coordinates. The wave amplitude and particle evolution include all finite Larmour radius effects. We describe and benchmark the currently implemented Alfvén eigenmode workflow, demonstrating correct particle motion, linear and nonlinear power transfer. The formulation and numerical scheme are sufficiently general as to allow easy future implementation of different kinds of eigenmodes, such as modes close to the ion-cyclotron frequency. The code can model multiple eigenmodes and multiple fast ion species simultaneously, and supports the general form of the equilibrium distribution in constants of motion.

Introduction

For tokamaks to allow reactor relevant regimes of operation, a proportion of the confined plasma must necessarily be comprised of energetic ions. The anticipated abundance of non-Maxwellian alpha particles in the burning plasma regime on ITER would be both a key physics achievement and a new stability consideration. It is well understood, both from current experiments and significant theoretical study, that fast particles can resonantly destabilise wave eigenmodes in the bulk thermonuclear tokamak plasma, which can degrade performance and damage the plasma-facing components through energetic ion redistribution and loss.

Existing experiments with neutral beam injection (NBI) and ion cyclotron resonant heating (ICRH) have confirmed the destabilization of predicted bulk plasma eigenmodes such as the toroidal Alfvén eigenmode (TAE) [1] or the reverse shear Alfvén eigenmode (RSAE)[2]. In addition to the well-understood Alfvénic modes in the bulk plasma, wave activity in the ion-cyclotron range has also been observed, as well as lower frequency energetic particle modes (EPM) [3] which are thought to be large coherent motions of the fast-particles themselves interacting with a broad Alfvén continuum. A number of stability modelling strategies have been employed with varying levels of self-consistency and difficulty [4].

For the Alfvénic modes that have been identified as eigenmodes of the bulk plasma, very good agreement has been shown between the linear MHD theory and the observations [5]. This experimental fact is a powerful motivation for a general perturbative nonlinear predictive code for wave-particle interaction, where all the nonlinearity is assumed to be due to the perturbed fast ions rather than the bulk plasma. The perturbative approach is fundamentally the same as the nonlinear Landau damping solution given by O'Neil [6] and Mazitov [7] and later applied to Alfvén waves in the fusion context by Berk and Breizman[8], where particle orbits in tokamak geometry were computed using a guiding centre drift model with a simplified Alfvén wave expression [9]. The formulation of a Hamiltonian theory of guiding centre motion in realistic magnetic geometry [10] allowed similar

solutions of the drift-kinetic-Maxwell problem in codes such as ORBIT [11], FAC [12] and HAGIS [13]. All these codes relied on a delta-f scheme [14] , forcing the identically zero equilibrium contribution to the power transfer to be ignored in the marker population, improving Monte Carlo statistics in the remaining contribution coming from the perturbation.

In this work, we present the new HALO (HAgis LOcust) code, which is a full orbit implementation of the perturbative delta-f approach, allowing nonlinear modelling of any bulk plasma eigenmode at arbitrary frequency using the Vlasov-Maxwell system of equations. The high performance LOCUST-GPU code [15] serves as the orbit following foundation for the wave-particle physics described in this paper.

Physical model

In this section, we rederive a perturbative wave-particle treatment for a general Vlasov-Maxwell system and an associated delta-f noise reduction scheme. Our goal is to make the derivation sufficiently general to be useful to those working in both astrophysical and laboratory plasmas, as well as to make the orderings required for the perturbative approach as transparent as possible. We deviate from the usual variational approach [9] and instead start with Maxwell's equations.

Derivation of wave evolution equations

Starting with the Fourier transformed wave-equation

$$-\frac{c^2}{\omega^2}\boldsymbol{\nabla}\times\boldsymbol{\nabla}\times\tilde{\mathbf{E}}(\mathbf{x},\omega)+\tilde{\mathbf{E}}(\mathbf{x},\omega)=-\frac{i\mu_0 c^2}{\omega}\tilde{\mathbf{J}}(\mathbf{x},\omega) \tag{1}$$

we identify a Hermitian linear response portion $\int d\boldsymbol{x}'\,\boldsymbol{\sigma}(\boldsymbol{x},\boldsymbol{x}',\omega)\tilde{\mathbf{E}}(\boldsymbol{x}',\omega)$ of the total current density, and separate it from the anti-Hermitian linear $\tilde{\mathbf{J}}_{\bar{\sigma}}(\mathbf{x},\omega)$, nonlinear $\tilde{\mathbf{J}}_{\boldsymbol{NL}}(\mathbf{x},\omega)$ and free current $\tilde{\mathbf{J}}_{free}(\mathbf{x},\omega)$

$$\begin{aligned}&-\frac{c^2}{\omega^2}\boldsymbol{\nabla}\times\boldsymbol{\nabla}\times\tilde{\mathbf{E}}(\mathbf{x},\omega)+\tilde{\mathbf{E}}(\mathbf{x},\omega)\\&=-\frac{i\mu_0 c^2}{\omega}\left[\int d\boldsymbol{x}'\,\boldsymbol{\sigma}(\boldsymbol{x},\boldsymbol{x}',\omega)\tilde{\mathbf{E}}(\boldsymbol{x}',\omega)\;+\tilde{\mathbf{J}}_{\boldsymbol{NL}}(\mathbf{x},\omega)+\tilde{\mathbf{J}}_{free}(\mathbf{x},\omega)+\tilde{\mathbf{J}}_{\bar{\sigma}}(\mathbf{x},\omega)\right]\end{aligned} \tag{2}$$

This rearrangement has been expressed a number of equivalent ways in the literature [16][17]

such as

$$K(\boldsymbol{x},\boldsymbol{x}',\omega)=\frac{\boldsymbol{\epsilon}(\boldsymbol{x},\boldsymbol{x}',\omega)}{\epsilon_0}=\left(\delta(\boldsymbol{x}-\boldsymbol{x}')\mathbf{I}+\frac{i\mu_0 c^2}{\omega}\boldsymbol{\sigma}(\boldsymbol{x},\boldsymbol{x}',\omega)\right) \tag{3}$$

$$\Lambda(\boldsymbol{x},\boldsymbol{x}',\omega)=\left[-\frac{c^2}{\omega^2}\delta(\boldsymbol{x}-\boldsymbol{x}')\boldsymbol{\nabla}\times\boldsymbol{\nabla}\times+K(\boldsymbol{x},\boldsymbol{x}',\omega)\right] \tag{4}$$

We will adopt the notation of Breizman et al. [18] making all terms have dimensions of current density

$$g\equiv-\frac{\omega}{i\mu_0 c^2}\Lambda \tag{5}$$

$$\int d\boldsymbol{x}'\,\mathrm{g}(\boldsymbol{x},\boldsymbol{x}',\omega)\tilde{\mathbf{E}}(\boldsymbol{x}',\omega)=\left(\tilde{\mathbf{J}}_{\boldsymbol{NL}}(\mathbf{x},\omega)+\tilde{\mathbf{J}}_{free}(\mathbf{x},\omega)+\tilde{\mathbf{J}}_{\bar{\sigma}}(\mathbf{x},\omega)\right) \tag{6}$$

Consider the linear homogeneous (undriven) MHD equation

$$\int d\boldsymbol{x}'\,\mathrm{g}_{\mathrm{MHD}}(\boldsymbol{x},\boldsymbol{x}',\omega)\tilde{\mathbf{E}}(\mathbf{x}',\omega)=0 \tag{7}$$

This formalism supports any Hermitian model for the plasma dielectric, so it is not restricted to just linear MHD. However, given the examples in this paper deal with shear Alfvén waves, we will label the linear response with "MHD" for the purposes of this derivation, however we will drop the label outside this derivation in order to avoid the implication that it *has* to be MHD.

The corresponding inhomogeneous (driven) MHD problem is

$$\int d\boldsymbol{x}'\, \mathrm{g}_{\mathrm{MHD}}(\boldsymbol{x},\boldsymbol{x}',\omega)\tilde{\mathbf{E}}(\mathbf{x}',\omega) = \tilde{\mathbf{J}}_{free}(\mathbf{x},\omega) \tag{8}$$

The free currents are independent of the electric field (by definition). If the drive from free currents is sufficiently weak, then solutions to an externally driven inhomogeneous equation at ω near ω' will resemble a homogeneous solution at ω'. We thus assume $|\omega| \gg |\omega - \omega'|$

$$\mathrm{g}_{\mathrm{MHD}}(\boldsymbol{x},\boldsymbol{x}',\omega) \approx \mathrm{g}_{\mathrm{MHD}}(\boldsymbol{x},\boldsymbol{x}',\omega') + \epsilon\left[(\omega-\omega')\frac{\partial}{\partial\omega}\right]\mathrm{g}_{\mathrm{MHD}}(\boldsymbol{x},\boldsymbol{x}',\omega') \tag{9}$$

where we have introduced the formal small ordering parameter ϵ which is the ratio of driving current to the dielectric currents

$$\frac{|\omega-\omega'|}{|\omega|} \sim \frac{\left|\tilde{\mathbf{J}}_{free}(\mathbf{x},\omega)\right|}{\left|\int d\boldsymbol{x}'\, \mathrm{g}_{\mathrm{MHD}}(\boldsymbol{x},\boldsymbol{x}',\omega)\tilde{\mathbf{E}}(\mathbf{x}',\omega)\right|} \ll 1 \tag{10}$$

We include ϵ simply as a label to remind the relative sizes of various terms, which should be set $\epsilon = 1$ to obtain the physical formulas.

The weakly driven MHD problem becomes

$$\int d\boldsymbol{x}'\left[\mathrm{g}_{\mathrm{MHD}}(\boldsymbol{x},\boldsymbol{x}',\omega') + \epsilon\left[(\omega-\omega')\frac{\partial \mathrm{g}_{\mathrm{MHD}}(\boldsymbol{x},\boldsymbol{x}',\omega')}{\partial\omega}\right]\right]\tilde{\mathbf{E}}(\mathbf{x}',\omega) = \epsilon\tilde{\mathbf{J}}_{free}(\mathbf{x},\omega) \tag{11}$$

The weakly driven MHD problem outlined above is analogous to certain classes of wave-particle problems where the currents are not free. In these problems, the plasma response currents are dominated by a linear Hermitian operator whose eigenfunctions are known, and the remaining nonlinear and anti-Hermitian response currents are deemed much smaller in comparison

$$\int d\boldsymbol{x}'\left[\mathrm{g}_{\mathrm{MHD}}(\boldsymbol{x},\boldsymbol{x}',\omega') + \epsilon\left[(\omega-\omega')\frac{\partial}{\partial\omega}\right]\mathrm{g}_{\mathrm{MHD}}(\boldsymbol{x},\boldsymbol{x}',\omega')\right]\tilde{\mathbf{E}}(\mathbf{x}',\omega) = \epsilon\tilde{\mathbf{J}}_{\boldsymbol{NL}}(\mathbf{x},\omega) + \epsilon\tilde{\mathbf{J}}_{\bar{\sigma}}(\mathbf{x},\omega) \tag{12}$$

$$\frac{|\omega-\omega'|}{|\omega|} \sim \frac{\left|\tilde{\mathbf{J}}_{\bar{\sigma}}(\mathbf{x},\omega)\right|}{\left|\int d\boldsymbol{x}'\, \mathrm{g}_{\mathrm{MHD}}(\boldsymbol{x},\boldsymbol{x}',\omega)\tilde{\mathbf{E}}(\mathbf{x}',\omega)\right|} \sim \frac{\left|\tilde{\mathbf{J}}_{\boldsymbol{NL}}(\mathbf{x},\omega)\right|}{\left|\int d\boldsymbol{x}'\, \mathrm{g}_{\mathrm{MHD}}(\boldsymbol{x},\boldsymbol{x}',\omega)\tilde{\mathbf{E}}(\mathbf{x}',\omega)\right|} \ll 1 \tag{13}$$

These orderings must be motivated by the specific wave phenomena being studied (see appendix for TAE discussion). The weak current sources depend on the electric field, so to form a closed system for the electric field, the relationship between the current sources and the electric field must be known.

We now seek to solve the wave equation for the nonlinear interaction of resonant fast particles. We combine the source currents into one term $\tilde{\mathbf{J}}_{\boldsymbol{fast}}(\mathbf{x},\omega)$

$$\int d\boldsymbol{x}' \left[\mathrm{g}_{\mathrm{MHD}}(\boldsymbol{x},\boldsymbol{x}',\omega') + \epsilon \left[(\omega-\omega')\frac{\partial}{\partial\omega} \right] \mathrm{g}_{\mathrm{MHD}}(\boldsymbol{x},\boldsymbol{x}',\omega') \right] \tilde{\mathbf{E}}(\mathbf{x}',\omega) = \epsilon \tilde{\mathbf{J}}_{\boldsymbol{fast}}(\mathbf{x},\omega) \tag{14}$$

Note the subtle difference between demanding that the fast particle contribution be small and the weaker assumption that the resonant and nonlinear contribution be small. It is well known that MHD is not sufficient to describe the Hermitian motion of fast particles, since particles can drift from flux surfaces. Care must be taken not to double count Hermitian current contributions in any choice of bulk plasma model. This so-called 'adiabatic' contribution is discussed in the appendix.

Exploiting the property that $\int d\boldsymbol{x}'\, \mathrm{g}_{\mathrm{MHD}}(\boldsymbol{x},\boldsymbol{x}',\omega')$ is a Hermitian operator with electric field eigenmodes $\boldsymbol{e}(\boldsymbol{x},\omega';\omega_j)$, we may multiply by any adjoint eigenmode $\boldsymbol{e}^{\dagger}(\boldsymbol{x},\omega';\omega_j)$

$$\int d\boldsymbol{x} \int d\boldsymbol{x}'\, \boldsymbol{e}^{\dagger}(\boldsymbol{x}';\omega_j)\delta(\omega'-\omega_j) \left[(\omega-\omega')\frac{\partial}{\partial\omega} \right] \mathrm{g}_{\mathrm{MHD}}(\boldsymbol{x},\boldsymbol{x}',\omega')\tilde{\mathbf{E}}(\mathbf{x}',\omega) = \delta(\omega'-\omega_j) \int d\boldsymbol{x}\, \boldsymbol{e}^{\dagger}(\boldsymbol{x};\omega_j)\tilde{\mathbf{J}}_{\boldsymbol{fast}}(\mathbf{x},\omega) \tag{15}$$

Integrating and performing the inverse transform

$$\int d\boldsymbol{x} \int d\boldsymbol{x}'\, \boldsymbol{e}^{\dagger}(\boldsymbol{x}';\omega_j) \left[\frac{\partial \mathrm{g}_{\mathrm{MHD}}(\boldsymbol{x},\boldsymbol{x}',\omega_j)}{\partial\omega} \left(\frac{\partial \tilde{\mathbf{E}}(\mathbf{x}',t)}{\partial \mathrm{t}} + i\omega_j \tilde{\mathbf{E}}(\mathbf{x}',t) \right) \right] = -i \int d\boldsymbol{x}\, \boldsymbol{e}^{\dagger}(\boldsymbol{x};\omega_j)\tilde{\mathbf{J}}_{\boldsymbol{fast}}(\mathbf{x},\mathrm{t}) \tag{16}$$

Using the completely general simplifying form $\tilde{\mathbf{E}}(\boldsymbol{x}',t) = \mathrm{A}(\mathrm{t};\omega_j)\tilde{\mathbf{E}}(\boldsymbol{x}')\boldsymbol{e}^{-i\omega_j \mathrm{t}}$

$$\int d\boldsymbol{x} \int d\boldsymbol{x}'\, \boldsymbol{e}^{\dagger}(\boldsymbol{x}';\omega_j) i \frac{\partial \mathrm{g}_{\mathrm{MHD}}(\boldsymbol{x},\boldsymbol{x}',\omega_j)}{\partial\omega} \tilde{\mathbf{E}}(\boldsymbol{x}')\, \dot{A}(t;\omega_j) = \int d\boldsymbol{x}\, \boldsymbol{e}^{i\omega_j \mathrm{t}} \boldsymbol{e}^{\dagger}(\boldsymbol{x};\omega_j)\tilde{\mathbf{J}}_{\boldsymbol{fast}}(\mathbf{x},\mathrm{t}) \tag{17}$$

The unknown mode structure $\boldsymbol{E}(\boldsymbol{x})$ can always be represented by a linear combination of eigenmodes because they form a complete orthogonal basis. By exploiting the orthogonality of the eigenfunctions, we obtain an ordinary differential equation for the amplitude and phase of an eigenmode normalised to the mode energy

$$\dot{A}(t;\omega_j) = -\frac{1}{2\delta W_{MHD}} \boldsymbol{e}^{i\omega_j \mathrm{t}} \int d\boldsymbol{x}\, \boldsymbol{e}^{\dagger}(\boldsymbol{x};\omega_j)\tilde{\mathbf{J}}_{\boldsymbol{fast}}(\boldsymbol{x},\mathrm{t}) \tag{18}$$

$$\delta W_{MHD} = -\frac{i}{2} \int d\boldsymbol{x} d\boldsymbol{x}'\, \boldsymbol{e}^{\dagger}(\boldsymbol{x};\omega_j) \frac{\partial \mathrm{g}_{\mathrm{MHD}}(\boldsymbol{x},\boldsymbol{x}',\omega_j)}{\partial\omega}\, \boldsymbol{e}(\boldsymbol{x}';\omega_j) \tag{19}$$

This equation relates the linear growth of the wave energy with the instantaneous power transfer to the particles

$$\mathrm{A}(t;\omega_j) = Ce^{(\gamma - \mathrm{i}\Delta\omega)t}, \Re e\left\{\frac{\dot{A}}{A}\right\} = \gamma_L + \gamma_{NL}(t) \tag{20}$$

$$P \equiv \mathfrak{R}e\left\{ A^* \boldsymbol{e}^{i\omega_j \mathrm{t}} \int d\boldsymbol{x} \left(\boldsymbol{e}^{\dagger}(\boldsymbol{x};\omega_j)\tilde{\mathbf{J}}_{\boldsymbol{fast}}(\boldsymbol{x},\mathrm{t}) \right) \right\} \tag{21}$$

giving the well-known linear relationship when $\gamma_{NL}(t) = 0$

$$\gamma_L = -\frac{P}{2A^2 \delta W_{MHD}} \tag{22}$$

The solution of the wave-particle problem is thus reduced to choosing the most relevant eigenmodes of the bulk plasma $\boldsymbol{e}(\boldsymbol{x};\omega_j)$, computing the motion of the resonant particle population

$\tilde{\mathbf{J}}_{\boldsymbol{fast}}(\boldsymbol{x},\mathrm{t})$ in the presence of those eigenmodes, and evolving the amplitude and phase of those modes $\mathrm{A}(\mathrm{t};\omega_j)$ in response to the normalized power transfer $\int d\boldsymbol{r}\left(\boldsymbol{e}^{i\omega_j \mathrm{t}}\boldsymbol{e}^{\dagger}(\boldsymbol{x};\omega_j)\tilde{\mathbf{J}}_{\boldsymbol{fast}}(\boldsymbol{x},\mathrm{t})\right)$ in inverse proportion to the mode energy δW_{MHD}.

Mode energy for TAE problems

For a cold plasma in the MHD ordering, the linear shear Alfvén response manifests as a polarization drift of ions on an equilibrium magnetic field and $E_{\parallel}=0$

$$\boldsymbol{v_p}(\boldsymbol{x},t)=\frac{d}{dt}\left(\frac{\boldsymbol{E}_{\perp}(\boldsymbol{x},t)}{\boldsymbol{B}(\boldsymbol{x})\Omega_c(\boldsymbol{x})}\right)=\frac{m_i}{e_i\boldsymbol{B^2}(\boldsymbol{x})}\frac{d\boldsymbol{E}_{\perp}(\boldsymbol{x},t)}{dt} \tag{23}$$

Staying within the linear approximation, we use the equilibrium density

$$n_i(\boldsymbol{x})\boldsymbol{v_p}(\boldsymbol{x},t)=\frac{n_i(\boldsymbol{x})m_i}{e\boldsymbol{B^2}(\boldsymbol{x})}\frac{d\boldsymbol{E}_{\perp}(\boldsymbol{x},t)}{dt} \tag{24}$$

Fourier transforming and identifying the Alfvén speed $v_A=\frac{B}{\sqrt{\mu_0 m_i n_i}}$, we obtain the appropriate generalized Ohm's law for the TAE

$$\boldsymbol{J_{TAE}}(\boldsymbol{x},\omega)=\int d\boldsymbol{x}'\left(-i\omega\frac{1}{\mu_0}\delta(\boldsymbol{x}'-\boldsymbol{x})\frac{1}{v_A^2(\boldsymbol{x}')}\boldsymbol{E}_{\perp}(\boldsymbol{x}',\omega)\right) \tag{25}$$

$$\sigma_{TAE}(\boldsymbol{x},\boldsymbol{x}',\omega)=-i\omega\frac{1}{\mu_0}\delta(\boldsymbol{x}'-\boldsymbol{x})\frac{1}{v_A^2(\boldsymbol{x}')} \tag{26}$$

Using the definition of the wave equation

$$\frac{\partial \mathrm{g}_{\mathrm{TAE}}(\boldsymbol{x},\boldsymbol{x}',\omega)}{\partial\omega}=\frac{2i}{\mu_0 c^2}\delta(\boldsymbol{x}-\boldsymbol{x}')+\frac{2i}{\mu_0}\delta(\boldsymbol{x}'-\boldsymbol{x})\frac{1}{v_A^2(\boldsymbol{x}')} \tag{27}$$

The first term on the right-hand side of equation 27 corresponds to the displacement current which is smaller than the second term by $\frac{v_A^2}{c^2}$ and is neglected. Thus, we obtain the mode energy for the Shear Alfvén wave [19]

$$\delta W_{TAE}=\frac{1}{\mu_0}\int d\boldsymbol{x}\frac{\boldsymbol{e}^{\dagger}(\boldsymbol{x};\omega_j)\boldsymbol{e}(\boldsymbol{x};\omega_j)}{v_A^2(\boldsymbol{x})} \tag{28}$$

delta-f model for the fast current

Solving for the electric field in Maxwell's wave equation requires an evolution equation for the currents in self-consistent response to the field. Most of the current in the perturbative model is due to the linear dielectric currents of the non-resonant oscillatory plasma. For the TAE problem, this Hermitian current is calculated from the closed linear MHD equations.

The remaining fast current is responsible for resonant drive and damping of the mode. The fast current for a particle of charge Z*e* is obtained from the distribution function

$$\tilde{\mathbf{J}}_{\boldsymbol{fast}}(\boldsymbol{x},\mathrm{t})=\int d\boldsymbol{p}\, f(\boldsymbol{x},\boldsymbol{p},t)Ze\boldsymbol{v} \tag{29}$$

The motion of the fast particles is assumed satisfy a Hamiltonian $H(\boldsymbol{x},\boldsymbol{p},t)$ with a distribution that evolves according to a collisionless kinetic equation

$$\frac{\partial f(\boldsymbol{x},\boldsymbol{p},t)}{\partial t}+\frac{\partial}{\partial \boldsymbol{x}}\cdot\left(\frac{\partial H}{\partial \boldsymbol{p}}\,f(\boldsymbol{x},\boldsymbol{p},t)\right)-\frac{\partial}{\partial \boldsymbol{p}}\cdot\left(\frac{\partial H}{\partial \boldsymbol{x}}f(\boldsymbol{x},\boldsymbol{p},t)\right)=0 \tag{30}$$

$$\dot{\boldsymbol{x}}=\frac{\partial H}{\partial \boldsymbol{p}},\dot{\boldsymbol{p}}=-\frac{\partial H}{\partial \boldsymbol{x}} \tag{31}$$

It is useful to separate the distribution function and trajectories into equilibrium and perturbed components. Letting $f=F_0+\delta f, H=H_0+\delta H$

$$\frac{\partial(F_0+\delta f)}{\partial t}+\frac{\partial}{\partial \boldsymbol{x}}\left(\frac{\partial(H+\delta H)}{\partial \boldsymbol{p}}(F_0+\delta f)\right)-\frac{\partial}{\partial \boldsymbol{p}}\left(\frac{\partial(H+\delta H)}{\partial \boldsymbol{x}}(F_0+\delta f)\right)=0 \tag{32}$$

We assume the fast particles to be in equilibrium in the absence of waves

$$\frac{\partial}{\partial \boldsymbol{x}}\left(\frac{\partial H_0}{\partial \boldsymbol{p}}F_0\right)-\frac{\partial}{\partial \boldsymbol{p}}\left(\frac{\partial H_0}{\partial \boldsymbol{x}}F_0\right)=0 \tag{33}$$

Since the equilibrium is known, we seek an evolution equation for the unknown perturbed distribution δf, arriving at

$$\frac{\partial \delta f}{\partial t}+\frac{\partial}{\partial \boldsymbol{x}}\frac{\partial(H_0+\delta H)}{\partial \boldsymbol{p}}\delta f-\frac{\partial}{\partial \boldsymbol{p}}\frac{\partial(H_0+\delta H)}{\partial \boldsymbol{x}}\delta f=\frac{\partial}{\partial \boldsymbol{p}}\frac{\partial \delta H}{\partial \boldsymbol{x}}F_0-\frac{\partial}{\partial \boldsymbol{x}}\frac{\partial \delta H}{\partial \boldsymbol{p}}F_0 \tag{34}$$

The left-hand side is the time derivative of the perturbed distribution taken along perturbed Hamiltonian trajectories. The right-hand side is the source term that depends only on the perturbed forces and the initial equilibrium. The linear version of the initial value problem is recovered by following unperturbed orbits on the left-hand side of equation 34, retaining the perturbed Hamiltonian only in the source term on the right-hand side.

The perturbed forces are calculated from the wave equation forming a closed system of equations for the waves and the perturbed fast current.

Numerical method

delta-f scheme marker evolution

Using the discrete representation, the i^{th} marker is associated with a unique initial position in phase space (x_i,p_i)

$$\frac{\partial F_0}{\partial \boldsymbol{x}}(\boldsymbol{x},\boldsymbol{p},t)\approx\sum_i \delta(\boldsymbol{x}-\boldsymbol{x}(t;\boldsymbol{x_i},\boldsymbol{p_i}))\delta(\boldsymbol{p}-p(t;\boldsymbol{x_i},\boldsymbol{p_i}))\frac{\partial F_0}{\partial \boldsymbol{x}}(\boldsymbol{x},\boldsymbol{p})\Delta^3x_i\Delta^3p_i \tag{35}$$

$$\frac{\partial F_0}{\partial \boldsymbol{p}}(\boldsymbol{x},\boldsymbol{p},t)\approx\sum_i \delta(\boldsymbol{x}-\boldsymbol{x}(t;\boldsymbol{x_i},\boldsymbol{p_i}))\delta(\boldsymbol{p}-p(t;\boldsymbol{x_i},\boldsymbol{p_i}))\frac{\partial F_0}{\partial \boldsymbol{p}}(\boldsymbol{x},\boldsymbol{p})\Delta^3x_i\Delta^3p_i \tag{36}$$

$$\delta f(\boldsymbol{x},\boldsymbol{p},t)\equiv\sum_i \delta\big(\boldsymbol{x}-\boldsymbol{x}(t;\boldsymbol{x_i},\boldsymbol{p_i})\big)\delta\big(\boldsymbol{p}-p(t;\boldsymbol{x_i},\boldsymbol{p_i})\big)\delta f(\boldsymbol{x},\boldsymbol{p},t)\Delta^3x_i\Delta^3p_i \tag{37}$$

The volume spanned by a marker $\Delta^3x_i\Delta^3p_i$ is defined as the product of lengths taken from half-way between one adjacent marker to another adjacent marker at their initial positions in phase space. The volume is a constant of the motion due to the Hamiltonian nature of the orbits.

Inserting into the delta-f equation and integrating, we find

$$\delta\dot{f}(t;\boldsymbol{x_i},\boldsymbol{p_i})$$
$$=-\frac{\partial \delta H}{\partial \boldsymbol{p}}(t;\boldsymbol{x_i},\boldsymbol{p_i})\cdot\frac{\partial F_0}{\partial \boldsymbol{x}}(\boldsymbol{x}(t;\boldsymbol{x_i},\boldsymbol{p_i}),\boldsymbol{p}(t;\boldsymbol{x_i},\boldsymbol{p_i}))+\frac{\partial \delta H}{\partial \boldsymbol{x}}(t;\boldsymbol{x_i},\boldsymbol{p_i})\cdot\frac{\partial F_0}{\partial \boldsymbol{p}}(\boldsymbol{x}(t;\boldsymbol{x_i},\boldsymbol{p_i}),\boldsymbol{p}(t;\boldsymbol{x_i},\boldsymbol{p_i})) \tag{38}$$

we simplify the notation re-writing equation 38 as

$$\delta\dot{f}_i(t) = -\delta\dot{\boldsymbol{x}}_{\boldsymbol{i}}(t)\cdot\left(\frac{\partial F_0}{\partial \boldsymbol{x}}\right)_p\left(\boldsymbol{x}_{\boldsymbol{i}}(t),\boldsymbol{p}_{\boldsymbol{i}}(t)\right) - \delta\dot{\boldsymbol{p}}_{\boldsymbol{i}}(t)\cdot\left(\frac{\partial F_0}{\partial \boldsymbol{p}}\right)_x\left(\boldsymbol{x}_{\boldsymbol{i}}(t),\boldsymbol{p}_{\boldsymbol{i}}(t)\right) \tag{39}$$

For the Maxwell-Vlasov system in HALO, we transform to more convenient variables(x, v) found in the Vlasov equation. The Jacobian between coordinate systems is a constant

$$\left|\frac{\partial(\boldsymbol{x},\boldsymbol{p})}{\partial(\boldsymbol{x},\boldsymbol{v})}\right| = m^3 \tag{40}$$

Thus, we may immediately rescale our distribution functions to those found in the Vlasov equation and perform a point transformation. The right-hand side is a dot product of a tangent vector with a gradient. Such a product is covariant with respect to arbitrary changes in coordinate basis, thus we may rewrite

$$\delta\dot{f}_i(t) = -\delta\dot{\boldsymbol{x}}_{\boldsymbol{i}}(t)\cdot\left(\frac{\partial F_0}{\partial \boldsymbol{x}}\right)_{\boldsymbol{v}}\left(\boldsymbol{x}_{\boldsymbol{i}}(t),\boldsymbol{v}_{\boldsymbol{i}}(t)\right) - \delta\dot{\boldsymbol{v}}_{\boldsymbol{i}}(t)\cdot\left(\frac{\partial F_0}{\partial \boldsymbol{v}}\right)_{\boldsymbol{x}}\left(\boldsymbol{x}_{\boldsymbol{i}}(t),\boldsymbol{v}_{\boldsymbol{i}}(t)\right) \tag{41}$$

It is straightforward to explicitly obtain $\delta\dot{x}(x,v,t)$ and $\delta\dot{v}(x,v,t)$ from the phase-space Lagrangian of full-orbit particle motion

$$L(\boldsymbol{x},\boldsymbol{v},\dot{\boldsymbol{x}},\dot{\boldsymbol{v}},t) = (m\boldsymbol{v} + e\boldsymbol{A_0} + e\boldsymbol{\delta A})\cdot\dot{\boldsymbol{x}} - \left(e\Phi_0 + e\delta\Phi + \frac{m}{2}\boldsymbol{v}\cdot\boldsymbol{v}\right) \tag{42}$$

The Euler-Lagrange equations give the perturbed portion of the force in phase space

$$\delta\dot{\boldsymbol{x}}(\boldsymbol{x},\boldsymbol{v},t) = 0 \tag{43}$$

$$\delta\dot{\boldsymbol{v}}(\boldsymbol{x},\boldsymbol{v},t) = \frac{e}{m}(\boldsymbol{v}\times\delta\boldsymbol{B} + \delta\boldsymbol{E}) \tag{44}$$

The general form of the 2D equilibrium distribution function assuming no equilibrium electric field is

$$F_0 = \sum_{sgn(v_\parallel)} F(E,\mu,P_\phi;sgn(v_\parallel)) \tag{45}$$

$$n(\boldsymbol{x}) = \sum_{sgn(v_\parallel)}\int d\boldsymbol{v}\, F(E,\mu,P_\phi;sgn(v_\parallel)) \tag{46}$$

where the invariants of motion energy E, gyroinvariant μ and toroidal canonical momentum P_ϕ and $sgn(v_\parallel)$ label each possible equilibrium orbit. The nature of an equilibrium is that it is a function of the unperturbed field and unperturbed particle orbits. Therefore, the coordinate mapping we require is from the space (x,v,t) to the space of invariants of the unperturbed motion. Perturbed fields do not appear in these equilibrium invariants, it is only the trajectories that are perturbed.

$$F_0 = F\left(E\left(\boldsymbol{x}_{\boldsymbol{i}}(t),\boldsymbol{v}_{\boldsymbol{i}}(t)\right),\mu\left(\boldsymbol{x}_{\boldsymbol{i}}(t),\boldsymbol{v}_{\boldsymbol{i}}(t)\right),P_\phi\left(\boldsymbol{x}_{\boldsymbol{i}}(t),\boldsymbol{v}_{\boldsymbol{i}}(t)\right);sgn(v_\parallel(0))\right) \tag{47}$$

$$P_\phi(\boldsymbol{x},\boldsymbol{v}) = mRv_\phi + Ze\psi_0(x) \tag{48}$$

$$E(\boldsymbol{x},\boldsymbol{v}) = \frac{1}{2}mv^2 \tag{49}$$

$$\mu(\boldsymbol{x},\boldsymbol{v}) = \frac{\frac{1}{2}mv_\perp^2}{B_0(\boldsymbol{x})} + O\left(\frac{\rho}{L}\right) \tag{50}$$

where we have written only the lowest order in gyroradius expansion $\frac{\rho}{L}$ for the gyroinvariant.

Applying the chain rule to the equilibrium equation we arrive at our delta-f scheme in cylindrical coordinates

$$\delta\dot{f}_i(t) = -\delta\dot{v}_R\left[mv_R\left(\frac{\partial F_0}{\partial E}\right)_{\mu,P_\phi} + \frac{\partial\mu}{\partial v_R}\left(\frac{\partial F_0}{\partial\mu}\right)_{E,P_\phi}\right]$$

$$-\delta\dot{v}_Z\left[mv_Z\left(\frac{\partial F_0}{\partial E}\right)_{\mu,P_\phi}+\frac{\partial\mu}{\partial v_Z}\left(\frac{\partial F_0}{\partial\mu}\right)_{E,P_\phi}\right]$$

$$-\delta\dot{v}_\phi\left[mv_\phi\left(\frac{\partial F_0}{\partial E}\right)_{\mu,P_\phi}+mR\left(\frac{\partial F_0}{\partial P_\phi}\right)_{\mu,E}+\frac{\partial\mu}{\partial v_\phi}\left(\frac{\partial F_0}{\partial\mu}\right)_{E,P_\phi}\right] \tag{51}$$

with all quantities understood to be measured along a marker trajectory $(\boldsymbol{x_i}(t), \boldsymbol{v_i}(t))$. When $\frac{\omega}{\Omega} \ll 1$ as expected for low-n shear Alfvén waves, the gyro-invariant μ contributions to δf are assumed zero and we may set terms containing $\frac{\partial}{\partial\mu} \approx 0$ and $\mu(t) = \mu(0)$.

Now we obtain an explicit expression for the work done by the wave on the delta f markers

$$f(\boldsymbol{x},\boldsymbol{v},t) \approx \sum_i \delta\big(\boldsymbol{x}-\boldsymbol{x_i}(t)\big)\,\delta\big(\boldsymbol{v}-\boldsymbol{v_i}(t)\big)\big(F_0(\boldsymbol{x},\boldsymbol{v})+\delta f_i(t)\big)\Delta^3x_i\Delta^3v_i \tag{52}$$

$$\tilde{\mathbf{J}}_{\boldsymbol{fast}}(\boldsymbol{x},\mathrm{t}) = e\sum_i \boldsymbol{v_i}\delta\big(\boldsymbol{x}-\boldsymbol{x_i}(t)\big)(F_0(\boldsymbol{x},\boldsymbol{v_i})+\delta f_i(t))\Delta^3x_i\Delta^3v_i \tag{53}$$

$$\dot{A}\big(t;\omega_j\big) = -\frac{1}{\delta W_{TAE}}e^{i\omega_j\mathrm{t}}\,e\sum_i \boldsymbol{e}^{\dagger}\big(\boldsymbol{x_i}(t);\omega_j\big)\cdot\boldsymbol{v}_i\big[F_0\big(\boldsymbol{x_i}(t),\boldsymbol{v_i}(t)\big)+\delta f_i(t)\big]\,\Delta^3x_i\Delta^3v_i \tag{54}$$

In a 2-D equilibrium, the function $F_0(x,v)$ is axisymmetric, which implies that we have contributions from the equilibrium proportional to $\int d\phi cosn\phi$ which vanish identically. Dropping the equilibrium contribution therefore reduces the noise significantly, owing to the smallness of δf when compared with F_0.

$$\dot{A}\big(t;\omega_j\big) = -\frac{1}{2\delta W}e^{i\omega_j\mathrm{t}}\,e\sum_i \boldsymbol{e}^{\dagger}\big(\boldsymbol{x_i}(t);\omega_j\big)\boldsymbol{v}_i\delta f_i(t)\,\Delta^3x_i\Delta^3v_i \tag{55}$$

$$\delta\boldsymbol{E}\big(\boldsymbol{x},t;\omega_j\big) = A\big(t;\omega_j\big)\boldsymbol{e}\big(\boldsymbol{x};\omega_j\big)e^{-i\omega_j t} \tag{56}$$

Applications

MHD eigenmodes from MISHKA for TAE studies

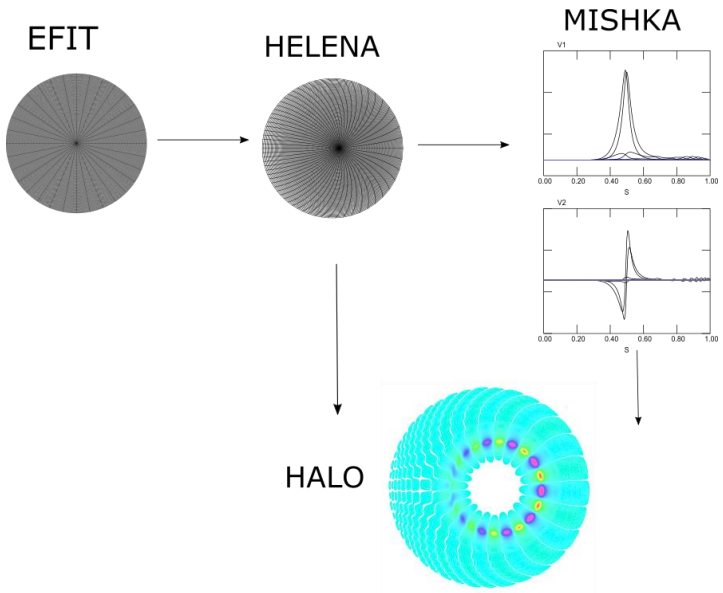

Figure 1: Alfvénic workflow currently implemented in HALO

The Alfvénic eigenmode workflow currently implemented in HALO is shown schematically in Figure 1 and is the basis for the examples presented in the rest of this paper. A solution to the Grad-Shafranov equation in cylindrical coordinates is first obtained either via a reconstruction process from experiment via EFIT [20], by prediction, or by postulate. In particular, the profiles $p(\psi)$ and $FF(\psi)$ and the location of the boundary is required. With the equilibrium profiles and boundary known, a second solution of the Grad-Shafranov equation must be obtained in a straight-field line coordinate system using the HELENA [21] code. This solution produces a high-fidelity equilibrium reconstruction suitable for linear MHD analysis, as well as a coordinate mapping between the cylindrical and straight field line coordinate systems. The high-fidelity equilibrium is provided to the MISHKA [22] linear MHD code and a set of eigenmodes of interest are computed.

The MISHKA eigenmodes are represented with the perturbed fluid velocity in the straight field-line coordinates(s, θ, φ). For ideal modes, MISHKA outputs two variables (v_1, v_2) where v_1 is related to the contravariant radial (s) component of the perturbed flow velocity $\tilde{V}$ and v_2 is related to $\hat{V}^2 = [\tilde{V} \times B_0]_1$

$$v_1(s,\theta,\varphi) = e^{\lambda t} e^{in\varphi} \sum_m e^{im\theta} \sum_{i=1}^{N} \left(v_{m,i}^1 H^1(s) + dv_{m,i}^1 H^2(s) \right) \tag{57}$$

$$v_2(s,\theta,\varphi) = e^{\lambda t} e^{in\varphi} \sum_m e^{im\theta} \sum_{i=1}^{N} \left(v_{m,i}^2 h^1(s) + dv_{m,i}^2 h^2(s) \right) \tag{58}$$

where the second summation is over radial grid points. The radial dependence is represented using Hermite polynomial basis functions of which there are two per radial grid point. For reasons of pollution avoidance v_1 is expressed in terms of cubic Hermite polynomials $H^1(s)$ and $H^2(s)$ whereas v_2 is expressed in terms of quadratic polynomials $h^1(s)$ and $h^2(s)$ [21].

The non-zero covariant components of the vector potential relate to the velocity components and in-turn the electric and magnetic fields in straight-field line coordinates

$$J = \frac{d\psi}{ds}\frac{qR^2}{RB_\phi} \tag{59}$$

$$A_1 = \frac{-iv_2}{\lambda} \tag{60}$$

$$\frac{d\psi}{ds} q\hat{A}_2 = -\frac{v_1}{\lambda} \tag{61}$$

$$\hat{A}_2 \equiv [\boldsymbol{A} \times \boldsymbol{B_0}]^1 / \boldsymbol{B_0^2}. \tag{62}$$

$$J\delta B^1 = -i\left(m\left(\frac{d\psi}{ds}\hat{A}_2\right) + n\left(\frac{d\psi}{ds} q\hat{A}_2\right)\right) \tag{63}$$

$$J\delta B^2 = inA_1 + \frac{\partial}{\partial s}\left(\frac{d\psi}{ds}\hat{A}_2\right) \tag{65}$$

$$J\delta B^3 = \frac{\partial}{\partial s}\left(\frac{d\psi}{ds} q\hat{A}_2\right) - imA_1 \tag{66}$$

$$\delta E_i = -\frac{\lambda A_i}{c} \tag{67}$$

The straight field line representation of the eigenmode is then transformed to conventional cylindrical coordinates using the mapping and metric tensor provided from HELENA. Note that the variables used in MISHKA as repeated above are expressed in cgs Gaussian units, whereas in the rest of the paper we have employed S.I. units.

Benchmark case: alpha particle driven TAE

For benchmarking and demonstration purposes, an alpha-particle-driven unstable TAE test case was contrived based on a circular equilibrium, with parameters comparable to existing large tokamak experiments.

Parameter	Value
$\epsilon = a/R_0$	0.25
$v_A/2a\Omega_c$	0.03
R_0	3.0m
B_0	3.0T
D:T (%)	50:50
q_0	1.82
q_{95}	3.31
T_e	20keV
T_i	20keV
$n_\alpha(0)\,/n_e(0)$	1%

Table 1: Parameters chosen for alpha particle driven TAE case

For simplicity, equilibrium flux functions were polynomials adjusted by hand in HELENA to give a monotonic q-profile with an $n = 6$ TAE found with MISHKA at $s \approx 0.5$, and temperature and density profiles were assumed flat.

Although HALO supports input of arbitrary fast ion distribution functions of the equilibrium form $F(E, \mu, P_\phi; sgn(v_\parallel))$, the alpha particle distribution was taken to be $F = \alpha(E)\gamma(P_\phi)$ with polynomial $\gamma(P_\phi) \propto \left(1 - \overline{P_\phi}^2\right)^{10}$ and slowing down distribution [23][12]

$$\alpha(E) \propto \frac{1}{v^3 + v_c^3}\,\mathrm{Erfc}\left[\frac{E - 3.5\mathrm{MeV}}{106 \times 10^3\sqrt{T_i[\mathrm{keV}]}}\right]$$
$$v_c \equiv \left(3\sqrt{\pi}\frac{m_e Z_1}{4}\right)^{\frac{1}{3}}\sqrt{\frac{2T_e}{m_e}}$$
$$Z_1 = \frac{0.5}{2m_p} + \frac{0.5}{3m_p} \tag{68}$$

Particle orbit test: wave-particle trapping of resonant orbits comparison with HAGIS

To solve the coupled Maxwell-Vlasov system, the fast particle response to the waves must be faithfully represented. The fields must satisfy Maxwell's equations, and the particles must move according to the Lorentz force law. Equivalently, particles must be shown to move according to the phase-space Lagrangian Equation 42.

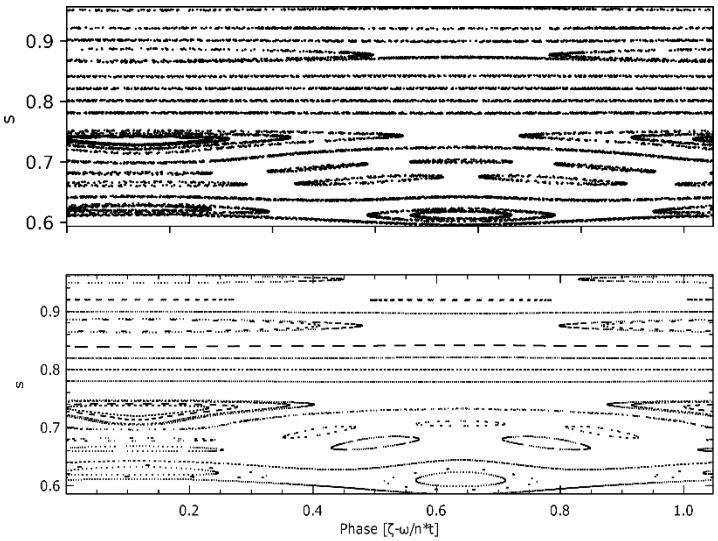

Figure 2: Comparison of Poincaré plots produced by HALO (top) and HAGIS (bottom). Resonant orbits at critical locations become trapped in the wave forming islands.

To test the fast particle response to the eigenmodes, a set of alpha particle markers at different radial locations were launched in the presence of the benchmark $n = 6$ TAE with a fixed mode amplitude $\frac{dB_r}{B_0} = 3 \times 10^{-3}$. All particles were loaded as deeply co-passing $\mu = 0$ and with the same velocity matching the Alfvén speed at the magnetic axis. Both HAGIS and HALO were run recording particle position and wave phase over many orbits, to identify resonantly trapped alpha particle islands in phase space. The comparison of orbits given by the two codes is given in Figure 2and shows excellent qualitative agreement.

A more quantitative test comes from conserving the invariant

$$K = E - \frac{\omega}{n} P_\phi \tag{69}$$

This is a particularly stringent test that particles follow orbits derived from the Lagrangian Equation 42 because it relates the time and spatial derivatives of the perturbing fields to each other through

$$\frac{d}{dt} E = -\frac{\partial L}{\partial t} \tag{70}$$

$$\frac{d}{dt} P_\phi = \frac{\partial L}{\partial \phi} \tag{71}$$

The radial excursions shown in Figure 2 imply a corresponding change in toroidal canonical momentum due to a breaking of axisymmetry. Figure 3 shows that although the mode is varying the test particle canonical momentum by up to 10%, the invariant is found to be conserved to better than $\frac{\Delta K}{K} \sim 1 \times 10^{-5}$.

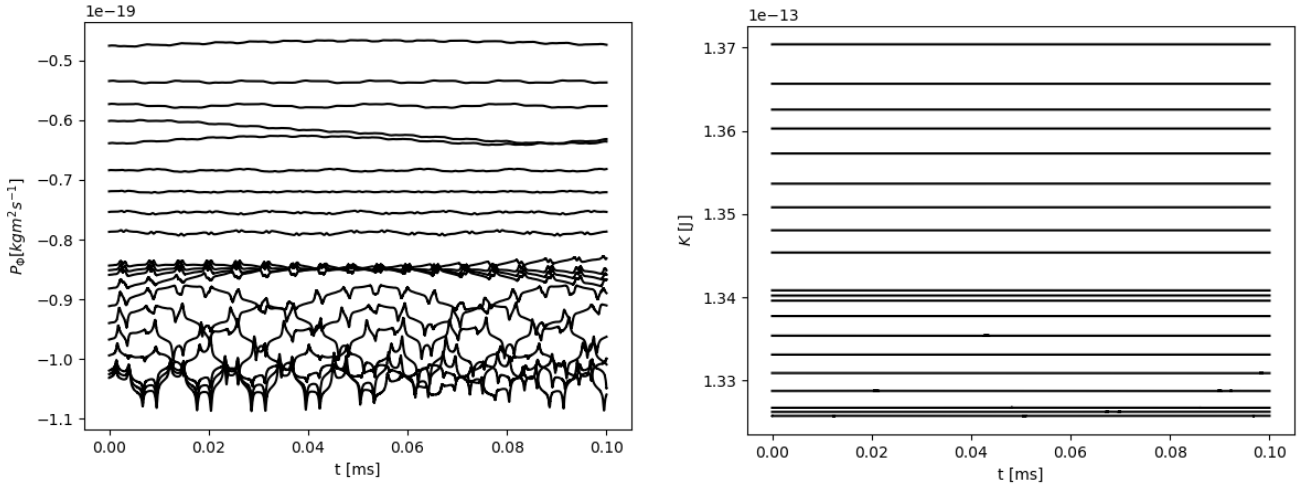

Figure 3: Variation in toroidal canonical momentum for test particle orbits (left) and the preservation of wave invariant K (right).

Stability test: linear growth-rate comparison with HAGIS

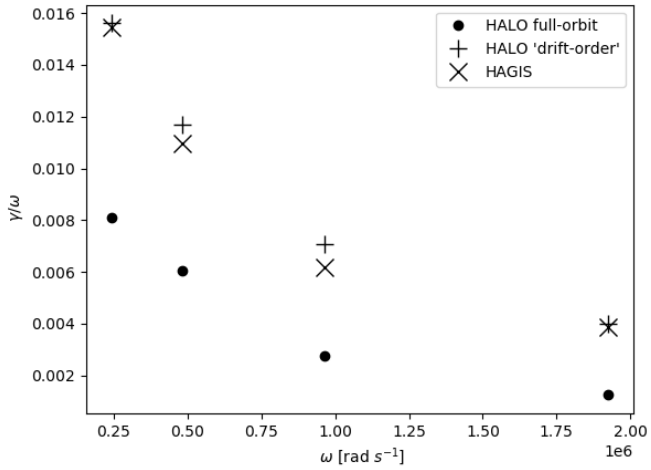

Figure 4: Comparison of linear growth rates between HAGIS and HALO, varying the mode frequency

Spatial gradients in the particle distributions are a source of free energy for TAEs that propagate in the fast ion-diamagnetic direction due to a universal instability drive [24], with drive occurring if

$$\omega < n\omega_* = n\frac{\partial F/\partial P_\phi}{\partial F/\partial E} \tag{72}$$

The temporal evolution of the TAE is characterised initially by a linear phase where the mode is governed by exponential growth. In this phase, the mode energy is small when compared with the free energy in the gradients. Moreover, the fields of the mode are sufficiently small as to not significantly perturb the equilibrium orbits of the resonant particles.

A scan of frequency for the TAE benchmark case was run in both the HALO and HAGIS codes, and a comparison of the measured linear growth rates is shown in Figure 4. The linear growth rates in HALO show roughly a factor 2 reduction in drive compared with the HAGIS drift calculation. The difference in drive between HAGIS and HALO lies in the drift approximation for the power transfer evaluating the electric field at the average guiding centre rather than the rapidly varying instantaneous particle location

$$\dot{A}_{\boldsymbol{HAGIS}}(t;\omega_j) = -\frac{1}{2\delta W}e^{i\omega_j t}\, e\sum_i \boldsymbol{e}^{\dagger}(\boldsymbol{X_i}(t);\omega_j)\boldsymbol{V}_i\delta f_i(t)\,\Delta^3 x_i\Delta^3 v_i$$
$$\boldsymbol{x} \equiv \boldsymbol{X} + \boldsymbol{\rho}$$
$$\boldsymbol{V} \equiv \dot{\boldsymbol{X}} \tag{73}$$

The drift-kinetic, gyrokinetic [25][26] and quasi-linear [27] theories can be obtained by gyroaveraging the Vlasov equation over the rapid gyration timescales, resulting in equations in terms of the guiding centre position. Although the guiding centre drift velocity is a good approximation to the average motion of the particles, the field evaluated at the guiding centre is not a good approximation for the average field. At frequencies much lower than the cyclotron frequency, both the gyrokinetic and quasi-linear equations for the perturbed distribution function include terms lacking in the drift theory proportional to $J_0(k_\perp\rho)$ which captures the finite Larmor radius (FLR) effect of the decreased average electric field experienced by the particle. A simple calculation shows that such a decrease in drive is to be expected for the benchmark case; $k_\perp \approx \frac{m}{r} \approx \frac{12.5}{0.4}$, and at the Alfvén speed $\rho \approx 0.045m$ giving $J_0(k_\perp\rho)$ =0.57.

For the sole purpose of comparison with the linear HAGIS results, a "drift-order" mode in HALO was implemented, where the electric field in the power transfer Equation 55 was modified to be evaluated at the guiding centre position

$$\boldsymbol{e}^{\dagger}\left(\boldsymbol{x_i}(\boldsymbol{t});\omega_j\right) \rightarrow \boldsymbol{e}^{\dagger}\left(\boldsymbol{X_i}(t);\omega_j\right) \tag{74}$$

giving good agreement in Figure 4.

Note that before any attempt is made to include this finite Larmor radius correction in a drift-kinetic code such as HAGIS, a technical point worth mentioning here is that the drift velocity $\boldsymbol{V}_i$ in guiding centre codes should be computed to one-higher order in Larmor radius for the resulting power transfer to be consistent with the 1st order drift-kinetic equation, owing to the charge of the particle appearing in the fast particle power transfer $\delta E \cdot \delta j$ [28]. This technical point is the reason for traditional drift-kinetic power calculations being formulated through the pressure rather than the electric field.

Nonlinear tests: mode saturation and frequency chirping due to phase space holes and clumps

The long-term nonlinear behaviour of the wave-particle system relies on solving the initial value problem for both wave evolution and particle evolution. The verification of linear growth rate implies that the power transfer between waves and particles is correct in the linear phase. We have also shown that test particle orbits are correctly perturbed by a finite mode and are resonantly trapped in the wave.

What remains to be shown is that there is sufficient temporal and spatial resolution in order to faithfully compute the wave power transfer in the nonlinear phase, conserving total energy.

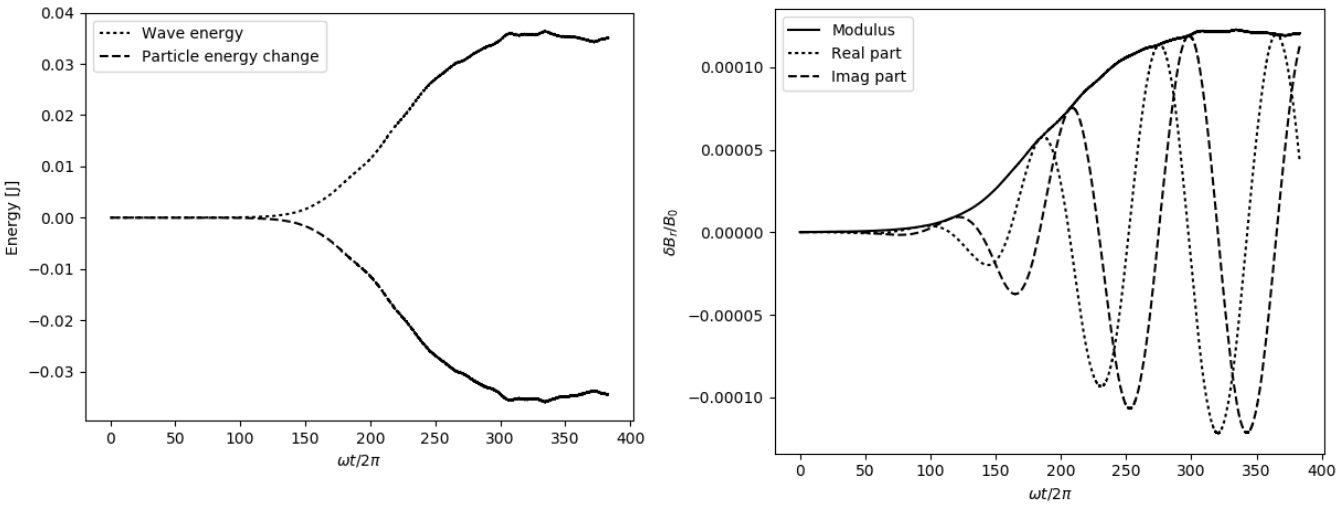

Figure 5: Nonlinear growth and saturation of the TAE (right) , and comparison between change in wave energy and sum of change in particle energy (left).

The long-term nonlinear behaviour of the TAE alpha-particle benchmark is given in Figure 5, showing the classic growth and saturation expected, and the conservation of energy between waves and particles. As the field grows, particle orbits deviate significantly from equilibrium orbits and can become resonantly trapped within the wave potential. The field energy grows as A^2, whereas the region in phase space that can supply energy grows approximately as $A^{3/2}$. When the two energies become comparable, the exponential growth slows until saturation when the gradients in the distribution are removed via phase-mixing of trapped orbits on a timescale comparable with the nonlinear bounce frequency [6].

A further test of nonlinear evolution is the creation of Bernstein-Greene-Kruskal (BGK) nonlinear waves that chirp in frequency. These holes and clumps in phase-space result from the shearing of trapped particle islands as the amplitude of the saturated state is modulated by damping [29][30].

A marginally unstable version of the TAE benchmark was created by considering an additional source current in the wave equation

$$\dot{A}(t;\omega_j) = -\frac{1}{2\delta W}\boldsymbol{e}^{i\omega_j \mathrm{t}} \int d\boldsymbol{x}\, \boldsymbol{e}^{\dagger}(\boldsymbol{x};\omega_j)\left[\tilde{\mathbf{J}}_{\boldsymbol{fast}}(\boldsymbol{x},\mathrm{t}) + \tilde{\mathbf{J}}_{\boldsymbol{d}}(\boldsymbol{x},\mathrm{t})\right] \tag{75}$$

this can be rewritten as an equation for the time varying growth-rate

$$\begin{aligned}\dot{A}(t;\omega_j) = \left(\gamma_{\mathrm{fast}}(\mathrm{t}) - \mathrm{i}\Delta\omega_{fast}(t)\right)A(t;\omega_j) \; + \\ \left(\gamma_d(\mathrm{t}) - \mathrm{i}\Delta\omega_d(t)\right)A(t;\omega_j)\end{aligned} \tag{76}$$

To produce nonlinear chirping, we assume a linear damping contribution $\gamma_d(\mathrm{t}) = \gamma_d,\ \Delta\omega_d(t) = 0$

$$\dot{A}(t;\omega_j) = -\frac{1}{2\delta W}\boldsymbol{e}^{i\omega_j \mathrm{t}} \int d\boldsymbol{x}\, \boldsymbol{e}^{\dagger}(\boldsymbol{x};\omega_j)\tilde{\mathbf{J}}_{\boldsymbol{fast}}(\boldsymbol{x},\mathrm{t}) + \gamma_d A(t;\omega_j) \tag{77}$$

The nonlinear TAE benchmark described earlier was repeated with a linear damping term included such that $\frac{\gamma_d}{\gamma_L} = 0.9$. Figure 6 gives the amplitude and frequency evolution of the marginally unstable evolution. The rapid amplitude modulation is typical of marginally stable TAE simulations performed with HAGIS [31] and with other codes [32]. Also evident is the expected steady production of BGK modes sweeping in frequency symmetrically above and below the eigenfrequency as expected from the bump-on-tail theory [33] and observed in previous TAE calculations [34] and has been observed in experiment [35].

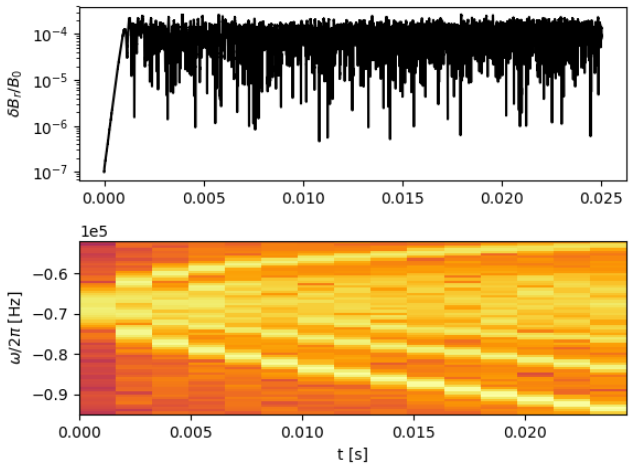

Figure 6: Amplitude (above) and Fourier spectrogram (below) of the TAE benchmark made marginally unstable.

Conserved quantities and convergence

The full-orbit motion of δf markers is described by the trajectories obtained from the Lagrangian given by Eqn. 42 as solved using the orbit-following portions of the LOCUST-GPU code [15] with either of the phase-volume preserving Boris or Strang particle orbit integrators [36].

For fully self-consistent HALO solutions, equations 51 and 55, as well as the particle trajectories specified by equation 42 are integrated simultaneously in time as an initial value problem. Particles are loaded in 5D phase space using a quasi-random Hammersley sequence [37] in order to reduce noise in the power transfer integral. Gyroangle is ignored in the loading scheme as it was expected that phase mixing would rapidly fill the remaining dimension. The rapid variation in the quantity $\boldsymbol{e}^{\dagger}(\boldsymbol{x_i}(t);\omega_j)\boldsymbol{v}_i$ governs the power transfer timescale, with only the drift contribution having any consequence for Alfvénic modes which oscillate on an $\omega \approx k_{\parallel} v_A$ timescale. Slower still is the growth time of $\dot{A}$ as dictated by the perturbative model. In order to integrate the rapidly varying power transfer between infrequent wave amplitude updates, a 6th order finite difference scheme was used.

The numerical scheme for coupled wave-particle solution has been tested for convergence in temporal and spatial integration and the results for the benchmark case are given in Figure 7. A time step of $1 \times 10^{-9} s$ in the benchmark problem corresponds to $\approx \frac{2\pi}{\Omega_c}\frac{1}{40}$ which is enough to solve the perturbed motion of the particles and conserve orbit invariant K, but appears insufficient in the continual time integration of power transfer $\boldsymbol{e}^{\dagger}(\boldsymbol{x_i}(t);\omega_j)\boldsymbol{v}_i$. Halving the timestep to $\approx \frac{2\pi}{\Omega_c}\frac{1}{80}$ for the 6th order scheme gives a dramatic improvement, with diminishing returns for further reductions. We have so far only attempted running LOCUST-GPU with simulations below 12 million particles, however we obtain convergence in global energy conservation at around 1 million particles.

Note the complete absence of any slowly growing or slowly decaying amplitude in the converged solution, which has been a stubborn feature in some other delta-f based results but one that we have been able to eliminate with high-order integration and sufficient statistics.

Also related to global energy conservation is the total particle conservation in the delta-f scheme. The perturbed distribution function δf represents the deviation of the distribution function from equilibrium and must therefore contain both positive and negative values as particles are moved from one area of phase space to another. Thus, exact particle number conservation would require that

$$\int d\boldsymbol{x}d\boldsymbol{v}\delta f = \sum \delta f_i \, \Delta^3 x_i \Delta^3 v_i = 0 \tag{78}$$

The total number of particles in the system includes the unperturbed particles as well as the perturbed particles and the fractional error in the total particle conservation is $\int d\boldsymbol{x}d\boldsymbol{v}\delta f / \int d\boldsymbol{x}d\boldsymbol{v}\, F_0$, however such a test is rather insensitive by virtue of the small proportion of particles involved in driving the mode, i.e. $\delta f \ll F_0$. A more stringent test $\int d\boldsymbol{x}d\boldsymbol{v}\delta f / \int d\boldsymbol{x}d\boldsymbol{v}\, |\delta f|$ is presented instead, which is a more direct measure of the error in the code as it computes wave-particle power transfer. The relative conservation of perturbed particles in Figure 7 implies a random fluctuation in the computed wave growth of the order of 1% with no systematic drift evident.

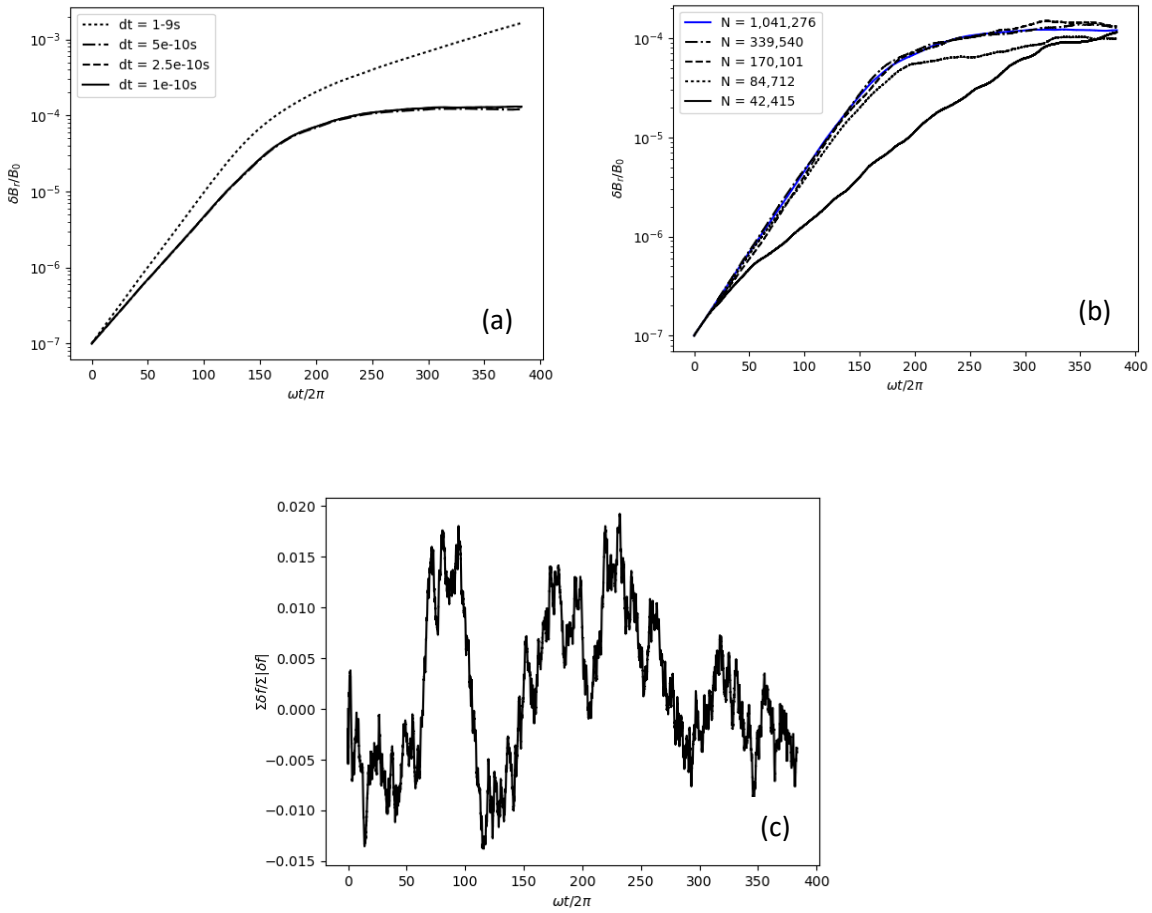

Figure 7: Convergence properties of the coupled wave-particle system. Plots of convergence with timestep (a) and number of markers (b) are shown, as well as the global conservation of particles in the delta-f scheme (c).

Conclusion and further work

We have presented the theory and validation of a new wave-particle code HALO which perturbatively solves the Maxwell-Vlasov problem when the nonlinearity is dominated by particle

currents that do not play a large role in the structure and frequency of the eigenmode. The approach generalizes the HAGIS code by allowing arbitrary particle motion in arbitrary geometry, interacting with eigenmodes whose frequencies are limited only by the particle integration timescale. The workflow currently implemented pertains to the TAE problem in tokamaks, however our presentation has been deliberately general so that this approach can be replicated easily for other kinds of bulk plasma modes.

For our TAE workflow, we have presented benchmarks against the drift-kinetic code HAGIS, with and without the new FLR corrections provided by HALO. The FLR corrections were found to be significant for an invented benchmark case with parameters that resemble current large tokamak experiments.

We plan to extend HALO to support workflows for modes other than the well-studied TAE problem, such as those located in the ion-cyclotron and ion-acoustic range of frequencies. It is likely that we will use the two-fluid extension to MISHKA, MISHKA3 [38], which includes the Hall-term required in the ion-cyclotron range of frequencies (see appendix), and for modes at low frequencies, viscous and heat flow effects.

The robustness of this method has undoubtedly been due in part to the Hamiltonian nature of the equations assumed. However it is well understood that the nonlinear evolution of TAEs seen in experiment requires collisions and sources/sinks to be modelled in order to reproduce all of the experimentally observed behaviour, including asymmetric frequency chirping [39]. Collisions have been implemented in various hybrid and gyrokinetic codes [40][41], but a fully consistent delta-f set of equations that includes collisions appears to be far from straightforward. This will likely be the focus of future work to complete the TAE model implemented in HALO.

Acknowledgments

The first author is grateful for the generous hospitality of the Institute for Fusion Studies at the University of Texas Austin which greatly facilitated the development of these ideas. This work has been carried out within the framework of the EUROfusion Consortium and has received funding from the Euratom research and training programme 2014-2018 and 2019-2020 under grant agreement No 633053 for the European Enabling Research Project WP17-ENR-MFE-CCFE-02 and from the RCUK Energy Programme (grant number EP/P012450/1). The views and opinions expressed herein do not necessarily reflect those of the European Commission. To obtain further information on the data and models underlying this paper please contact PublicationsManager@ukaea.uk.

Appendix A: Applicability to the TAE problem versus the EPM problem

TAE stability in a tokamak is a good example of a problem where the orderings used in HALO are valid. The weak currents not captured in the Hermitian MHD operator include the drive provided by fast particles, the linear damping provided by thermal ions, the linear damping provided by crossing of the continuum, and the nonlinear response. TAEs are discrete modes which exist in gaps in the Shear Alfvén continuum. They are weakly driven and damped and there is good experimental evidence for their mode structure resembling MHD solutions [5].

We turn our attention to the non-resonant nonlinear currents. The fluid current associated with the TAE mode is given by the polarization drift of ions

$$\boldsymbol{v_p}(\boldsymbol{x},t) = \frac{d}{dt}\left(\frac{\boldsymbol{E}_\perp(\boldsymbol{x},t)}{\boldsymbol{B}(\boldsymbol{x})\Omega_c(\boldsymbol{x})}\right) = \frac{m_i}{e_i \boldsymbol{B^2}(\boldsymbol{x})}\frac{d\boldsymbol{E}_\perp(\boldsymbol{x},t)}{dt} \qquad (A1)$$

$$\boldsymbol{v_p}(\boldsymbol{x},t)=\frac{m_i}{e_i|\boldsymbol{B}+\delta\boldsymbol{B}|^2}\frac{d\boldsymbol{E}_\perp}{dt}\approx\frac{m_i}{e_i(\boldsymbol{B^2}+\delta\boldsymbol{B^2})}\frac{d\boldsymbol{E}_\perp}{dt} \tag{A2}$$

$$\boldsymbol{v_p}(\boldsymbol{x},t)=\frac{m_i}{e_i}\frac{d\boldsymbol{E}_\perp}{dt}\left(\frac{1}{B^2}-\frac{\delta B^2}{B^4}+\cdots\right) \tag{A3}$$

The polarization drift is almost completely compressionless, so the polarization current depends on equilibrium ion density

$$\boldsymbol{J_p}(\boldsymbol{x},t)=\rho(\boldsymbol{x})\frac{d\boldsymbol{E}_\perp}{dt}\left(\frac{1}{B^2}-\frac{\delta B^2}{B^4}+\cdots\right) \tag{A4}$$

Identifying the linear and nonlinear responses

$$\frac{\left|\tilde{\mathbf{J}}_{\boldsymbol{NL}}\right|}{\left|\mathrm{g}_{\mathrm{MHD}}\tilde{\mathbf{E}}\right|}=\frac{\delta B^2}{B^2}+\cdots \tag{A5}$$

A fast particle driven TAE has a linear fast particle driven growth rate $\frac{\gamma}{\omega}$ ≈1% with a corresponding saturation amplitude of $\frac{\delta\boldsymbol{B}}{\boldsymbol{B}}\approx 0.1\%$. The perturbative approach which assumes a fixed mode structure is clearly a good approximation in such a regime and the fast particle nonlinearity is the dominant nonlinearity at least until mode saturation.

Conversely, energetic particle modes (EPMs) do not satisfy the perturbative orderings by definition[42][43] and are not valid modes to be considered self-consistently with HALO; specifically, the distribution function in the vicinity of the resonant velocity has strong gradients which produce currents that are responsible both for the drive of the modes as well as the modes' very existence. The coherent motion of the fast current does not merely provide an external drive, but rather, the coherent motion *is* the EPM

$$\frac{\left|\tilde{\mathbf{J}}_{\boldsymbol{NL}}\right|}{\left|\mathrm{g}_{\mathrm{MHD}}\tilde{\mathbf{E}}\right|}\sim 1 \tag{A6}$$

EPMs such as fishbones can also occur at low frequencies where strong damping interactions with the Alfvén continuum produce large response currents

$$\frac{\left|\tilde{\mathbf{J}}_{\bar{\sigma}}\right|}{\left|\mathrm{g}_{\mathrm{MHD}}\tilde{\mathbf{E}}\right|}\sim 1 \tag{A7}$$

The strong continuum damping implies a low-quality linear plasma response at the fishbone frequency. With such a broad bulk plasma response, discussion of a bulk plasma linear "mode" is meaningless.

Appendix B: Mode energy of modes in the ion-cyclotron range

Although this paper has focused on the TAE, HALO is sufficiently general to allow study of arbitrary perturbative eigenmodes. Here we give the derivation of $\frac{\partial g_{COLD}}{\partial\omega}$ required for dW_{COLD} which is valid for any cold plasma eigenmode below the electron cyclotron frequency.

The general cold plasma displacement velocity for a given particle species is [17]

$$\boldsymbol{v}(\boldsymbol{x},\omega)=i\frac{e}{m}\frac{\omega}{\omega^2-\Omega_{\mathrm{c}}(\mathbf{x})^2}\left(\boldsymbol{E}(\boldsymbol{x},\omega)-\frac{{\Omega_{\mathrm{c}}}^2(\boldsymbol{x})}{\omega^2}E_{\parallel}(\boldsymbol{x},\omega)\widehat{\boldsymbol{b}}(\boldsymbol{x})\right)$$
$$-\frac{\Omega_{\mathrm{c}}(\mathbf{x})^2}{\omega^2-\Omega_{\mathrm{c}}(\mathbf{x})^2}\frac{\boldsymbol{E}(\boldsymbol{x},\omega)\times\widehat{\boldsymbol{b}}}{B_0} \tag{A8}$$

Looking first at the electron current, for frequencies well below the electron cyclotron frequency

$$\boldsymbol{j_e}(\boldsymbol{x},\omega) = i\frac{n_e e^2}{m_e\omega}E_{\parallel}(\boldsymbol{x},\omega)\widehat{\boldsymbol{b}}(\boldsymbol{x}) - ne\frac{\boldsymbol{E}(\boldsymbol{x},\omega)\times\widehat{\boldsymbol{b}}(\boldsymbol{x})}{B_0} \tag{A9}$$

and for ions of charge Ze and cyclotron frequency Ω_{c}

$$\boldsymbol{j_i}(\boldsymbol{x},\omega) = i\frac{n_i Z^2 e^2}{m_i}\frac{\omega}{\omega^2-\Omega_{\mathrm{c}}(\mathbf{x})^2}\left(\boldsymbol{E}(\boldsymbol{x},\omega) - \frac{{\Omega_{\mathrm{c}}}^2(\boldsymbol{x})}{\omega^2}E_{\parallel}(\boldsymbol{x},\omega)\widehat{\boldsymbol{b}}(\boldsymbol{x})\right)$$
$$-n_i Ze\frac{\Omega_{\mathrm{c}}(\mathbf{x})^2}{\omega^2-\Omega_{\mathrm{c}}(\mathbf{x})^2}\frac{\boldsymbol{E}(\boldsymbol{x},\omega)\times\widehat{\boldsymbol{b}}}{B_0} \tag{A10}$$

Using quasi-neutrality we find, after some manipulation, that the total current is

$$\boldsymbol{j}(\boldsymbol{x},\omega) = -i\omega\frac{n_i m_i}{B_0^2}\frac{\Omega_{\mathrm{c}}^2}{\Omega_{\mathrm{c}}^2-\omega^2}\boldsymbol{E}_{\perp}(\boldsymbol{x},\omega) + \left(\frac{n_i Z^2 e^2}{m_i\omega}+\frac{ne^2}{m_e\omega}\right)iE_{\parallel}(\boldsymbol{x},\omega)\widehat{\boldsymbol{b}}(\boldsymbol{x})$$
$$+\frac{\omega^2}{\Omega_{\mathrm{c}}^2-\omega^2}\frac{ne}{B_0}\,\boldsymbol{E}_{\perp}(\boldsymbol{x},\omega)\times\widehat{\boldsymbol{b}}(\boldsymbol{x}) \tag{A11}$$

We can clearly identify a binormal Hall current which is out of phase with the polarization current. This Hall current is the additional physics required in dW_{COLD} that is ignored for Alfvénic modes. Decomposing the electric field along the orthogonal directions $\hat{e}_1, \hat{e}_2, \hat{b}$ we obtain the dielectric tensor $\sigma(\boldsymbol{x},\boldsymbol{x}',\omega)$ (cf. Shafranov [17]) defined through the generalized Ohm's law expression

$$\boldsymbol{j}(\boldsymbol{x},\omega) = \int \sigma(\boldsymbol{x},\boldsymbol{x}',\omega)\begin{pmatrix}E_1\\E_2\\E_{\parallel}\end{pmatrix}d^3\boldsymbol{x}' \tag{A12}$$

$$\sigma_{COLD}(\boldsymbol{x},\boldsymbol{x}',\omega) = \delta(\boldsymbol{x}-\boldsymbol{x}')\begin{pmatrix}A(\boldsymbol{x},\omega) & iH(\boldsymbol{x},\omega) & 0\\ -iH(\boldsymbol{x},\omega) & A(\boldsymbol{x},\omega) & 0\\ 0 & 0 & P(\boldsymbol{x},\omega)\end{pmatrix} \tag{A13}$$

where

$$A(\boldsymbol{x},\omega) = -i\omega\frac{n_i m_i}{B_0^2}\frac{\Omega_{\mathrm{c}}^2}{\Omega_{\mathrm{c}}^2-\omega^2} \tag{A14}$$

$$iH(\boldsymbol{x},\omega) = \frac{\omega^2}{\Omega_{\mathrm{c}}^2-\omega^2}\frac{ne}{B_0} \tag{A15}$$

$$P(\boldsymbol{x},\omega) = i\left(\frac{n_i Z^2 e^2}{m_i\omega}+\frac{ne^2}{m_e\omega}\right) \tag{A16}$$

Again, neglecting the displacement current means $g = -\sigma$. Taking the derivative of equation $A13$ gives

$$\frac{\partial g_{COLD}}{\partial \omega}(\boldsymbol{x},\boldsymbol{x}',\omega)=\delta(\boldsymbol{x}-\boldsymbol{x}')\begin{pmatrix} i\frac{1}{\mu_0}\frac{1}{v_A^2}\frac{\Omega_c^2(\Omega_c^2+\omega^2)}{(\Omega_c^2-\omega^2)^2} & -\frac{2\Omega_c^2\omega}{(\Omega_c^2-\omega^2)^2}\frac{ne}{B_0} & 0 \\ \frac{2\Omega_c^2\omega}{(\Omega_c^2-\omega^2)^2}\frac{ne}{B_0} & i\frac{1}{\mu_0}\frac{1}{v_A^2}\frac{\Omega_c^2(\Omega_c^2+\omega^2)}{(\Omega_c^2-\omega^2)^2} & 0 \\ 0 & 0 & i\left(\frac{n_iZ^2e^2}{m_i\omega^2}+\frac{ne^2}{m_e\omega^2}\right) \end{pmatrix} \quad (A17)$$

In the MHD limit $\omega \ll \Omega_c$, the off-diagonal Hall $H(\boldsymbol{x},\omega)$ contributions to the mode energy vanish leaving only the diagonal polarization drift found in Eqn. 28 for the perpendicular field.

Appendix C: The adiabatic contribution and the HAGIS and FAC expressions

In HALO, the perturbed distribution in Eqn. 55 contains both the real and imaginary components of the correction to frequency. The linear real contribution to the frequency from the imaginary power transfer is also known as the "fluid", "incompressible" or "adiabatic" part of δf [24]

$$\frac{d}{dt}\delta f_{adiabatic}(t)=\frac{d\delta P_\phi}{dt}\frac{\partial F}{\partial P_\phi}+e\frac{d\delta\Phi}{dt}\frac{\partial F}{\partial E}-\frac{d}{dt}\left(\mu\frac{\delta B}{B}\right)\frac{\partial F}{\partial \mu} \quad (A18)$$

$$\frac{d}{dt}\delta f(t)=\frac{d}{dt}\delta f_{adiabatic}(t)+\frac{d}{dt}h(t) \quad (A19)$$

where $h(t)$ is the usual label for the non-adiabatic contribution.

Both the HAGIS and FAC codes (as well as the linear CASTOR-K code [44]) explicitly ignore adiabatic contributions to the mode frequency and focus instead on computing the growth rate due to real power transfer. By using MHD for the mode structure, this implies that these codes are ignoring the fast particle pressure contributions to the mode structure and frequency. More recently, there has been work in combining the LIGKA code with HAGIS to weaken this assumption both linearly and nonlinearly [45].

We can re-obtain the non-adiabatic HAGIS/FAC evolution equations Eqn. 21 in [13] and Eqn. 29 in [12] by considering a low-β MHD approximation for an Alfvén eigenmode

$$\nabla\times\sum_m \alpha_m \boldsymbol{B_0}=\delta\boldsymbol{B} \quad (A20)$$

$$\alpha_m=\frac{k_{\parallel m}\delta\Phi_{\mathrm{m}}}{B_0\omega} \quad (A21)$$

The power transfer term in Eqn. 55 is then proportional to

$$\begin{aligned} e^{i\omega_j \mathrm{t}}\boldsymbol{e}^{\dagger}\left(\boldsymbol{x_i}(t);\omega_j\right)\boldsymbol{v} &= -\sum_m\left(\boldsymbol{v}\cdot\nabla\delta\Phi_{\mathrm{m}}^* e^{i\omega_j \mathrm{t}}+\boldsymbol{v}\cdot\frac{\partial}{\partial \mathrm{t}}\alpha_m^* e^{i\omega_j \mathrm{t}}\boldsymbol{B_0}\right) \\ &= -e^{i\omega_j \mathrm{t}}\sum_m\left(\boldsymbol{v}\cdot\nabla\delta\Phi_{\mathrm{m}}^*+i\omega v_\parallel\frac{k_{\parallel m}\delta\Phi_{\mathrm{m}}^*}{B_0\omega}\boldsymbol{B_0}\right) \end{aligned} \quad (A22)$$

Ignoring the adiabatic contribution implies

$$\frac{d\delta\Phi_{\mathrm{m}}^*}{dt}=\frac{\partial\delta\Phi_{\mathrm{m}}^*}{\partial t}+\boldsymbol{v}\cdot\nabla\delta\Phi_{\mathrm{m}}^*=0 \quad (A23)$$

Giving immediately the HAGIS/FAC results (in their notation)

$$A(t;\omega_j) \equiv X(t;\omega_j) - iY(t;\omega_j) \tag{A24}$$

$$S_{ijm} = \Im m\left\{e^{i(k_m\cdot x-\omega_j t)}\Phi_{\mathrm{m}}\right\} \tag{A25}$$

$$C_{ijm} \equiv \Re e\left\{e^{i(k_m\cdot x-\omega_j t)}\Phi_{\mathrm{m}}\right\} \tag{A26}$$

$$\dot{X}(t;\omega_j) = \frac{1}{2\delta W}e\sum_m\sum_i\left(k_{\|m}(\boldsymbol{x_i}(t))v_{\|i}(t)-\omega_j\right)S_{ijm}\delta f_i(t)\,\Delta^3x_i\Delta^3v_i \tag{A27}$$

$$\dot{Y}(t;\omega_j) = -\frac{1}{2\delta W}e\sum_m\sum_i\left(k_{\|m}(\boldsymbol{x_i}(t))v_{\|i}(t)-\omega_j\right)C_{ijm}\delta f_i(t)\,\Delta^3x_i\Delta^3v_i \tag{A28}$$

References

[1] Cheng C and Chance M 1986 Low-n Shear Alfvén Spectra in Axisymmetric Toroidal plasmas *Phys. Fluids* **29** 3695

[2] Berk H L, Borba D N, Breizman B N, Pinches S D and Sharapov S E 2001 Theoretical interpretation of Alfven cascades in tokamaks with nonmonotonic q profiles *Phys. Rev. Lett.* **87**

[3] Chen L 1994 Theory of magnetohydrodynamic instabilities excited by energetic particles in tokamaks *Phys. Plasmas* **1** 1519

[4] Lauber P 2013 Super-thermal particles in hot plasmas—Kinetic models, numerical solution strategies, and comparison to tokamak experiments *Phys. Rep.* **533** 33–68

[5] Van Zeeland M A, Kramer G J, Austin M E, Boivin R L, Heidbrink W W, Makowski M A, McKee G R, Nazikian R, Solomon W M and Wang G 2006 Radial Structure of Alfvén Eigenmodes in the DIII-D Tokamak through Electron-Cyclotron-Emission Measurements *Phys. Rev. Lett.* **97** 135001

[6] O'Neil T 1965 Collisionless Damping of Nonlinear Plasma Oscillations *Phys. Fluids* **8** 2255

[7] Mazitov R K 1965 On the damping of plasma waves *Prikl. Mekh. Tekhn. Fiz* **1** 27–31

[8] Berk H L and Breizman B N 1990 Saturation of a single mode driven by an energetic injected beam. III. Alfvén wave problem *Phys. Fluids B Plasma Phys.* **2** 2246

[9] Berk H L, Breizman B N and Pekker M S 1995 Simulation of Alfven-wave-resonant-particle interaction *Nucl. Fusion* **35** 1713–20

[10] White R and Chance M 1984 Hamiltonian guiding center drift orbit calculation for plasmas of arbitrary cross section *Phys. Fluids* **27** 2455

[11] Wu Y, White R B, Chen Y and Rosenbluth M N 1995 Nonlinear evolution of the alpha-particle-driven toroidicity-induced Alfvén eigenmode *Phys. Plasmas* **2** 4555

[12] Candy J, Borba D, Berk H L, Huysmans G T A and Kerner W 1997 Nonlinear interaction of fast particles with Alfvén waves in toroidal plasmas *Phys. Plasmas* **4** 2597

[13] Pinches S D, Appel L C, Candy J, Sharapov S E, Berk H L, Borba D, Breizman B N, Hender T C, Hopcraft K I, Huysmans G T A and Kerner W 1998 The HAGIS self-consistent nonlinear wave-particle interaction model *Comput. Phys. Commun.* **111** 133–49

[14] Candy J 1996 A Numerical Method for Solution of the Generalized Liouville Equation *J. Comput. Phys.* **129** 160–9

[15] Akers R J, Verwichte E, Martin T J, Pinches S D and Lake R 2012 GPGPU Monte Carlo calculation of gyro-phase resolved fast ion and n-state resolved neutral deuterium distributions . *39th EPS Conference & 16th Int. Congress on Plasma Physics* vol 12 pp 1–4

[16] Melrose D B 1986 *Instabilities in Space and Laboratory Plasmas* (Cambridge: Cambridge University Press)

[17] Shafranov V D 1967 Electromagnetic Waves in a Plasma *Reviews of Plasma Physics* (Boston, MA: Springer US) pp 1–157

[18] Breizman B N, Berk H L, Pekker M S, Porcelli F, Stupakov G V. and Wong K L 1997 Critical nonlinear phenomena for kinetic instabilities near threshold *Phys. Plasmas* **4** 1559–68

[19] Breizman B N and Sharapov S E 1995 Energetic particle drive for toroidicity-induced Alfven eigenmodes and kinetic toroidicity-induced Alfven eigenmodes in a low-shear tokamak *Plasma Phys. Control. Fusion* **37** 1057–74

[20] Lao L L, John H St., Stambaugh R D, Kellman A G and Pfeiffer W 1985 Reconstruction of current profile parameters and plasma shapes in tokamaks *Nucl. Fusion* **25** 1611–1622

[21] Huysmans G T A, Goedbloed J P and Kerner W 1991 Isoparametric Bicubic Hermite Elements for Solution of the Grad-Shafranov Equation *Int. J. Mod. Phys. C* **02** 371–6

[22] Mikhailovskii A B, Huysmans G T A, Kerner W O K and Sharapov S E 1997 Optimization of computational MHD normal-mode analysis for tokamaks *Plasma Phys. Reports* **23** 844–57

[23] Gaffey J D 1976 Energetic ion distribution resulting from neutral beam injection in tokamaks *J. Plasma Phys.* **16** 149

[24] Porcelli F, Stankiewicz R and Kerner W 1994 Solution of the drift-kinetic equation for global plasma modes and finite particle orbit widths *Phys. Plasmas* **1**

[25] Simakov A N and Catto P J 2005 Drift kinetic equation exact through second order in gyroradius expansion *Phys. Plasmas* **12** 1–9

[26] Qin H, Tang W M and Rewoldt G 1998 Gyrokinetic theory for arbitrary wavelength electromagnetic modes in tokamaks *Phys. Plasmas* **5** 1035

[27] Kennel C F and Engelmann F 1966 Velocity Space Diffusion from Weak Plasma Turbulence in a Magnetic Field *Phys. Fluids* **9** 2377

[28] Rosenbluth M N and Rostoker N 1959 Theoretical Structure of Plasma Equations *Phys. Fluids* **2** 23

[29] Dupree T H 1972 Theory of Phase Space Density Granulation in Plasma *Phys. Fluids* **15** 334

[30] Berk H L, Breizman B N and Petviashvili N V 1997 Spontaneous hole-clump pair creation in weakly unstable plasmas *Phys. Lett. A* **234** 213–8

[31] Fitzgerald M, Sharapov S E, Rodrigues P and Borba D 2016 Predictive nonlinear studies of TAE-induced alpha-particle transport in the Q = 10 ITER baseline scenario *Nucl. Fusion* **56** 112010

[32] Wong H V and Berk H L 1998 Growth and saturation of toroidal Alfvén eigenmode modes destabilized by ion cyclotron range of frequency produced tails *Phys. Plasmas* **5** 2781

[33] Lilley M K and Nyqvist R M 2014 On the Formation of Phase Space Holes and Clumps *Phys. Rev. Lett.* **112** 155002

[34] Pinches S D, Berk H L, Gryaznevich M P, Sharapov S E and Contributors J-E 2004 Spectroscopic determination of the internal amplitude of frequency sweeping TAE *Plasma Phys. Control. Fusion* **46** S47–57

[35] Gryaznevich M P and Sharapov S E 2006 Perturbative and non-perturbative modes in START and MAST *Nucl. FUSION* **46** S942–50

[36] Delzanno G L and Camporeale E 2013 On particle movers in cylindrical geometry for Particle-In-Cell simulations *J. Comput. Phys.* **253** 259–77

[37] Halton J H 1960 On the efficiency of certain quasi-random sequences of points in evaluating multi-dimensional integrals *Numer. Math.* **2** 84–90

[38] Mikhailovskii A 1998 Generalized MHD for numerical stability analysis of high-performance plasmas in tokamaks *Plasma Phys. Control. Fusion* **40** 1907

[39] Lilley M K, Breizman B N and Sharapov S E 2010 Effect of dynamical friction on nonlinear energetic particle modes *Phys. Plasmas* **17**

[40] Todo Y, Berk H L and Breizman B N 2012 Simulation of Alfvén eigenmode bursts using a hybrid code for nonlinear magnetohydrodynamics and energetic particles *Nucl. Fusion* **52** 033003

[41] Cole M D J, Biancalani A, Bottino A, Kleiber R, Könies A and Mishchenko A 2017 Toroidal Alfvén eigenmodes with nonlinear gyrokinetic and fluid hybrid models *Phys. Plasmas* **24** 022508

[42] Fasoli A, Gormenzano C, Berk H ., Breizman B, Briguglio S, Darrow D ., Gorelenkov N, Heidbrink W ., Jaun A, Konovalov S ., Nazikian R, Noterdaeme J-M, Sharapov S, Shinohara K, Testa D, Tobita K, Todo Y, Vlad G and Zonca F 2007 Chapter 5: Physics of energetic ions *Nucl. Fusion* **47** S264–84

[43] Zonca F and Chen L 2014 Theory on excitations of drift Alfvén waves by energetic particles. I. Variational formulation *Phys. Plasmas* **21**

[44] Borba D and Kerner W 1999 CASTOR-K: Stability Analysis of Alfvén Eigenmodes in the Presence of Energetic Ions in Tokamaks *J. Comput. Phys.* **153** 101–38

[45] Schneller M 2013 *Transport of Super-thermal Particles and their Effect on the Stability of Global Modes in Fusion Plasmas* (PhD Thesis: Technische Universität München)